SYNTHESIS AND CHARACTERIZATION OF TRANSITION METAL-SUBSTITUTED INDIUM THIOSPINELS AS INTERMEDIATE BAND MATERIALS FOR HIGH EFFICIENCY SOLAR CELLS

José C. Conesa[1], Raquel Lucena[1], Perla Wahnón[2], Pablo Palacios[2], Irene Aguilera[2]
[1]Instituto de Catálisis y Petroleoquímica, CSIC. [2]Instituto de Energía Solar, ETSI de Telecomunicación, UPM
[1]Marie Curie 2, Cantoblanco, 28049 Madrid, Spain. [2]Ciudad Universitaria s/n, 28040 Madrid, Spain

ABSTRACT: It was recently proposed that higher efficiency can be achieved in PV cells having a single-absorbent if for the latter an intermediate band (IB) material is used which contains a partially filled, isolated band within the gap of an otherwise normal semiconductor. In_2S_3 and related compounds in which octahedrally coordinated In is substituted by a light transition metal are IB material candidates according to solid state chemistry concepts, this having been confirmed by quantum calculations. Here materials of this type have been chemically synthesized in powder form using wet solvothermal methods. Especially for vanadium-substituted In_2S_3, incorporation of the metal into the lattice is supported by XRD and TEM data, and only minor oxidation of vanadium from the V^{III} state to the V^{IV} state is evidenced by EPR. New sub-bandgap features appear in the diffuse reflectance optical spectra upon incorporation of vanadium; these coincide with the spectra that had been predicted by the quantum calculations as corresponding to the IB electronic structure. The realization of the IB concept in a single compound, that furthermore should be easy to prepare in the form needed for PV thin film cells, is thus achieved for the first time.
Keywords: Indium sulphide, Intermediate Band, Spectral Response, Solvothermal Synthesis, Doping

1 INTRODUCTION

In recent years it has been proposed [1] that the insertion of an additional level (the intermediate band, IB) in the forbidden gap of a semiconductor can provide an additional path for exciting electrons from the valence band (VB) to the conduction band (CB), based on the absorption of two photons with energy lower than the energy gap E_g between the VB and the CB (Figure 1). This two-photon process would be similar to what happens in natural photosynthesis. By making a better use of the solar spectrum a higher current can be obtained without decrease in voltage, and consequently the efficiency can be increased. To achieve this result efficiently the IB of such material must fulfil some conditions: it should not overlap the VB nor the CB, should be partially filled by electrons and should have real band characteristics rather than behaving as an isolated discrete level, in order to avoid large recombination effects. The maximum ideal limit of the later is computed then to be 63.1 %, while the same limit for a single absorbent PV cell of the standard type would be around 41% [1]. Optimal E_g values lie around 1.95 eV if working in high concentration conditions [1], and around 2.4 eV if using no concentration [2].

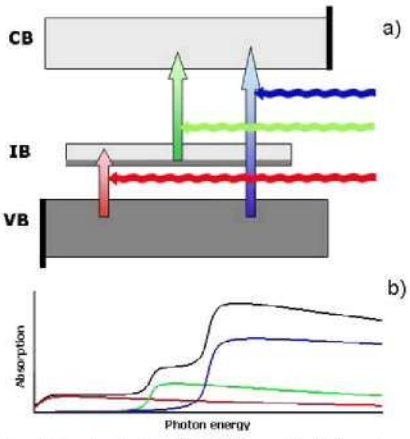

Fig. 1 The IB principle: a) photons of different energies promote electrons from the VB to the CB directly or *via* the IB, widening b) the photon range used.

Several compounds have been proposed for realizing the IB concept. Thus some experimentally prepared, highly mismatched II-VI or III-V alloys display spectral features that have been interpreted, using a band anticrossing model, in terms of an IB [3], although the degree of filling of the latter was not verified, nor first principles calculations were made. The present authors have proposed on the other hand, based on solid state chemistry concepts, that some tetrahedral polar semiconductors of types normally used in PV cells, as GaAs, GaP or $CuGaS_2$, can produce an IB electronic structure when the Ga atom in it is substituted partially by a light transition metal (TM) such as Ti or Cr [4,5,6].

Now we propose to use semiconductors having octahedral cations (to make easier their substitution by a TM), in particular the indium sulphides such as In_2S_3 which contain this element in octahedral sites. In such compounds the light TMs in octahedral coordination will split their d orbitals shell (presumed to be fully spin-polarized) to give a lowest 3-level manifold of t_{2g}-type symmetry. We choose thus Ti and V as TM elements for this substitution; these, having in the formal trivalent state respectively one and two 3d electrons, will have the mentioned lowest manifold partially filled. In_2S_3 is also particularly interesting because, besides having an appropriate band gap (E_g=2.0 eV [7]), its frequent use as buffer layer in thin film PV cells has led to the development of methods to deposit it in the convenient thin film form. As discussed below, calculations predict that by substitution with these TMs an IB structure forms, and after synthesizing such materials the optical spectra of some of them agree with the predictions of those calculations, evidencing that IB compounds with the required properties have been made for the first time. Further data on these systems are given elsewhere [8,9].

2 MATERIALS AND METHODS

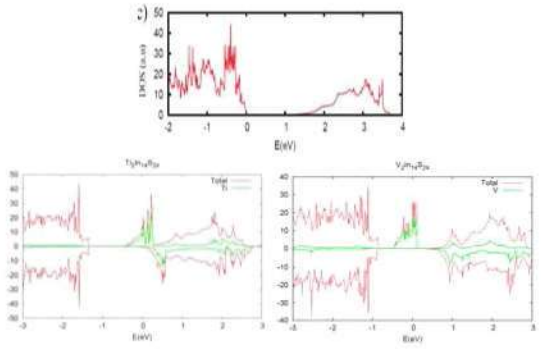

Fig. 2 DOS plots for In_2S_3-based materials: pure, Ti-doped and V-doped. Fermi level is at E=0. Green curves reflect atom-projected DOS.

2.1 Experimental

Solutions of appropriate proportions of $InCl_3$, $MgCl_2$, $ZnCl_2$, $TiCl_3$ and/or VCl_3 in water or water-ethylene glycol 1:9 mixtures were made, mixed under N_2 with solutions of NaS_2 or thiourea and heated at 463 K in a teflon-lined autoclave; then the powders obtained were washed with methanol and water and air-dried at 333 K.

XRD profiles were obtained with a Philips X´Pert Pro PANalytical diffractometer using Cu Kα radiation, TEM data with a JEOL 2100-F system having 0.19 nm point resolution and an EDS analyzer, and EPR and diffuse reflectance UV-Vis-NIR spectra with respectively a computer-interfaced Bruker ER200D system and a Varian Cary 5000 spectrophotometer using Spectralon® as reference material. For quantifying the number of spins detected in the EPR results (obtained as usual as first derivative of the absorption spectra), doubly integrated spectra were compared with that of a Cu^{2+} standard.

2.2 Calculation models and methods

Models for the calculations are based on the known structure of β-In_2S_3, a spinel in which cation vacancies, demanded by the stoichiometry of the compound, are ordered in tetrahedral sites to give a tetragonal centred lattice where the primitive cell content is $In_{16}S_{24}$ [10]. The TM-containing compounds models were derived from it substituting two of the octahedral In atoms in the primitive cell with the transition metal (Ti or V). It should be mentioned that some metastable phases of In_2S_3 exist [11], which contain as well most or all of indium in octahedral coordination; some calculations (not presented here) showed essentially no differences between the electronic structure of materials with these structures and those based on β-In_2S_3.

Spin-polarized DFT calculations were made with plane wave code VASP (v. 4.6) [12] at the GGA-PBE level, representing the atomic cores with the PAW method [13,14]. Crystal cell dimensions and atomic positions were always fully relaxed. The plane wave expansions of orbitals had a cutoff of 280 eV, and the Brillouin zones were sampled with a 4x4x4 Monkhorst-Pack mesh. From the converged Kohn-Sham wave-functions optical absorption spectra (only the direct transitions) were obtained [15].

3 RESULTS AND DISCUSSION

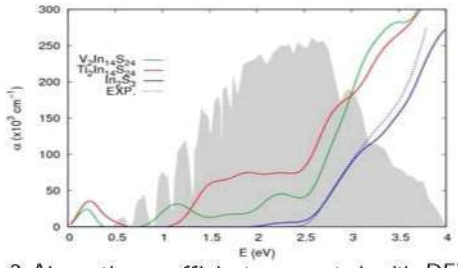

Fig. 3 Absorption coefficients computed with DFT for the systems indicated in Fig. 2. The solar spectrum is drawn as background. For In_2S_3 experimental data from [17] are displayed as well.

3.1 DFT predictions on In_2S_3-type materials

The DFT calculation made on TM-free In_2S_3 predicts a band gap of 0.86 eV. This value is lower than the experimental one (2.0 eV) as is typical of the DFT-GGA theory level. With the TM-containing systems the calculations produced always spin-polarized electronic structures. The resulting density of states (DOS) curves obtained for all cases are summarized in Fig. 2 (a more complete discussion and detailed band structures are given in [8]).

The incorporation of the TM into In_2S_3 is seen to introduce in the gap new features which are contributed mainly by the TM t_{2g}-type 3d orbitals (as shown by the projected DOS) and have band character and partial occupation. For TM=V the new band lies clearly isolated from the VB and CB, i.e. the desired IB characteristics are fulfilled. For TM=Ti it overlaps the CB, but this is due to the said underestimation of the main gap. As shown in other cases by calculations using the more accurate exact exchange method EXX [5,16], in the real materials the empty states but not the IB would be shifted to higher energies. If this shift (scissors operator) is made in the amount needed to make the pure semiconductor gap coincide with the experimental one, the TM-derived IB stands isolated also in this case.

Absorption curves computed from these results, after making this shift in the band structure, are given in Fig. 3. For the pure semiconductor the curves reproduce well the experimental data [17], which supports the validity of the method. For the doped materials absorption features at lower energies appear that can be related to the simplified scheme given in Fig. 1b. More detailed description and analysis are given in [8].

3.2 Synthesis and structural characterization of In_2S_3-type materials

Solvothermal synthesis of In_2S_3 in water produced a powder material with sharp X-ray diffraction (XRD) features (Fig. 4) that correspond to the α-In_2S_3 phase (which is the same as the β phase but with the tetrahedral vacancies disordered, so that a cubic spinel-like structure results [18]). When a mixed water-ethylene glycol solvent is used, the material is less crystallized and the metastable hexagonal γ phase appears as well.

The synthesis of the V-containing material required using the water-ethylene glycol solvent to avoid excessive oxidation of vanadium. The thus prepared material, in which the V:In ratio was 0.093:1 according to X-Ray fluorescence chemical analysis, displayed an XRD diagram where only features of the In_2S_3 phases appeared (Fig. 4). Examination of the material with HR-

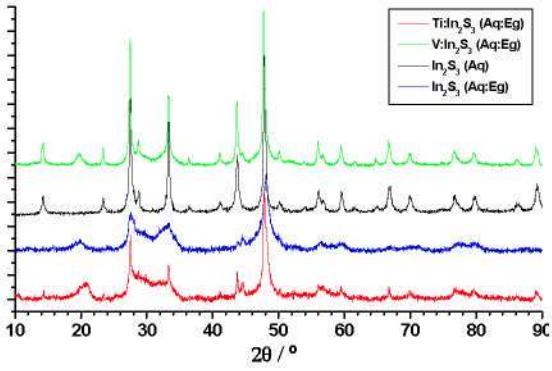

Fig. 4. XRD diagrams of In_2S_3 prepared in water and water-ethylene glycol, and of V- and Ti-containing In_2S_3 prepared in the latter solvent. All peaks except that at $2\theta \approx 20°$ (due to γ-In_2S_3) are from α-In_2S_3.

TEM (Fig. 5) showed the coexistence of well-crystallized domains, where lattice spacings corresponding to the spinel-type α-In_2S_3 structure could be detected. It is particularly worth noting that in some of these well-crystallized regions the EDS analysis indicated V:In ratios close to the bulk chemical analysis value, thus evidencing that vanadium had been able to enter the In_2S_3 lattice.

For the Ti-doped material, only less crystalline products could be obtained (see Fig. 4 for the XRD diagram of a material with Ti:In:S ratio = 0.21:1.79:3.2); it would seem thus that vanadium was more efficient in helping to nucleate the In_2S_3 phase in the mixed solvent.

3.3 Spectroscopic characterization of the materials

For the better crystallized V-containing product the EPR spectrum was recorded. As shown in Fig. 6 a signal, centred at $g \approx 1.98$, could be observed in which hyperfine structure can be discerned superimposed on a broader component. The temperature dependence of the spectrum follows a Curie-type behaviour, implying a paramagnetic character. The spectrum can be ascribed to V^{IV} species (V^{V} would be diamagnetic, and V^{III} species, with an even number of electrons, would not be observed in the spectrum). Integration of the spectrum allowed to determine quantitatively the amount of V^{IV} in the sample; it corresponded to 24% of the total amount of vanadium in it, evidencing that most of this element remained in the trivalent redox state.

UV-Vis-NIR spectra were recorded in the diffuse reflectance mode for the pure and TM-doped In_2S_3; they are presented in Fig. 7. While for In_2S_3 a clear jump at $E \approx 2.0$ eV is observed, which corresponds to the onset of

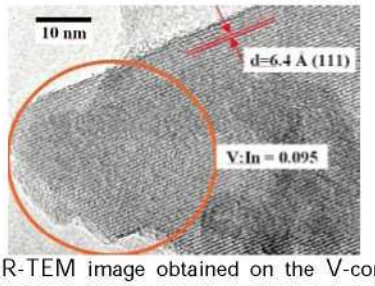

Fig. 5-HR-TEM image obtained on the V-containing In_2S_3 material. The V:In ratio shown, obtained with EDS, corresponds to the area marked with a circle.

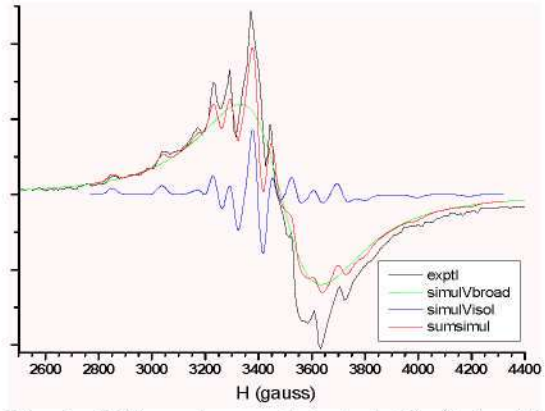

Fig. 6. EPR spectrum obtained at 77 K for V-substituted In_2S_3. Shown is its decomposition into a broadened signal and a well-resolved axial signal displaying hyperfine structure.

absorption at the bandgap energy, for the TM-containing materials absorption of photons with sub-bandgap energies is observed. In the case of the vanadium-containing sample this lower energy absorption appears clearly structured in two features: a jump at around 1.7 eV and a lower energy region that starts around 0.6 eV and rises gradually until it meets the mentioned jump. This structure is clearly similar, even if with less marked feature, to the absorption spectrum predicted by the DFT calculations for the V-substituted In_2S_3, presented in Fig. 3. The agreement between experimental and predicted spectrum shape is a strong indication that the desired V-substituted In_2S_3 material has been obtained, and that the electronic structure and optical characteristics of this compound indeed correspond to those foreseen for the sought IB material. Note that the observation of sub-bandgap optical absorption in both spectrum ranges (above and below ca. 1.7 eV) indicates, according to this model, that the IB is partially electron-filled, making possible both VB→IB and IB→VB transitions occur at finite rates. If the IB were either completely filled or empty only one sub-bandgap feature would be observed in the spectrum; this might be the case for the materials reported in [3].

For the Ti-substituted In_2S_3 sample giving the XRD profile shown in Fig. 4 the optical absorbance spectrum is given as well in Fig. 7. Sub-bandgap absorption is

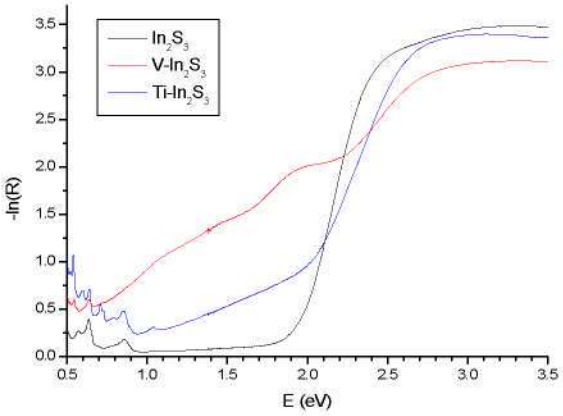

Fig. 7 Optical absorption diffuse reflectance spectra (presented as logarithm of the reflectance) obtained for the In_2S_3 materials (pure and substituted with V or Ti).

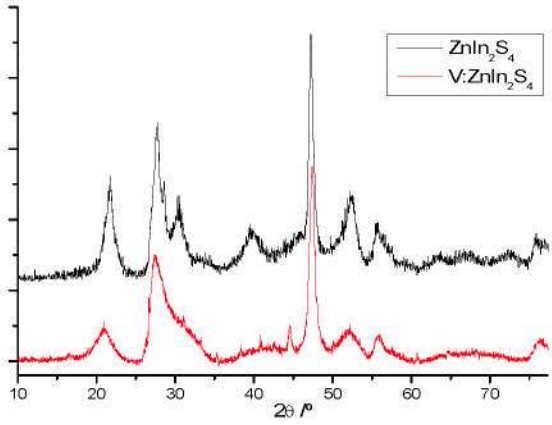

Fig. 8. XRD data of pure and V-substituted $ZnIn_2S_4$.

observed here as well, but it is much less structured, possibly due to the ill-crystallized nature of the material; the presence of an IB structure is thus less evident in this case.

3.4 Results on other In-based sulphides

Considering that the above described phenomenon of IB formation could be general in compounds of this class, synthesis of other octahedral In sulphide derived semiconductors, and TM substitution in them, has been undertaken. Some preliminary results on this system are here presented.

On the one hand, synthesis of $MgIn_2S_4$ was undertaken following the same solvothermal methods as in the previous cases. This compound has, like In_2S_3, a spinel structure, but with no cation vacancies; the spinel is largely inverse, i.e. most of the Mg ions lie in octahedral sites [19]. The bandgap is around 2.2 eV [20]. The obtained XRD diagrams and optical absorption spectra, as well as the results of DFT calculations, are similar (and are not being shown here) to those described above for the In_2S_3 case, suggesting that within the In thiospinel class of compounds the same IB features can be obtained.

Then the system based on $ZnIn_2S_4$ was tried. This is a hexagonal layered compound, existing in several stacking polytypes, where half of the In atoms are octahedrally coordinated, and the other half, as well as the Zn ions, are tetrahedrally coordinated [21]; its bandgap is 2.3 eV [22]. Following the same preparation methods as above, both pure $ZnIn_2S_4$ and the V-doped material were synthesized; atomic ratios in the products were Zn:In:S= 1:1.85:4 and Zn:V:In:S=1:0.2:1.8:3.96 respectively. XRD diagrams (Fig. 8) showed that these materials are moderately well crystallized powders (somewhat less in the case of the V-containing solid); only the diffraction lines corresponding to the layered $ZnIn_2S_4$ phase were found (the high pressure spinel phase [23] was not detected). Thus inclusion of V in the $ZnIn_2S_4$ lattice seems to have occurred. The raw diffuse reflectance spectra (Fig. 9) again show that upon inclusion of vanadium strong sub-bandgap absorption appears, and although it has less marked features that in the substituted In_2S_3 case a small shoulder at an energy ca. 0.5 eV lower than the main bandgap jump is discerned that might be due to an IB structure similar to that of the In_2S_3-based material. Its DFT modeling is in progress.

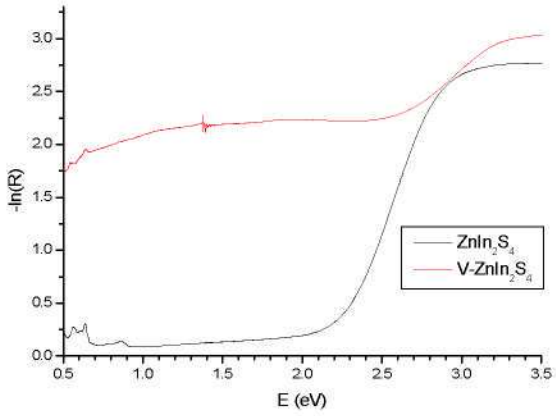

Fig. 9 Optical absorption diffuse reflectance spectra (presented as logarithm of the reflectance) obtained for the $ZnIn_2S_4$ materials (pure and substituted with V).

ACKNOWLEDGMENTS

This work was supported by the Spanish national funds through the Consolider Ingenio 2010 program (project GENESIS-FV, CSD2006-0004) and the National Research Plan (project CALIBAND, MAT2006-10618), by the European 6th Framework Programme (project FULLSPECTRUM, SES6-CT-2003-502620) and by the Community of Madrid (project NUMANCIA, S-05050/ENE/0310). R.L. thanks CSIC for a PhD grant of the I3P programme and I.A. thanks the MEC for a PhD grant of the FPU programme. Thanks are given to Dr. L. Pascual for help in obtaining the TEM data.

[1] A. Luque, A. Martí Phys. Rev. Lett. 78 (1997) 5014.
[2] A. Martí *et al.* J. Appl. Physics 103 (2008) 073706
[3] a) K.M., Yu *et al.* J. Appl. Phys. 95 (2004) 6232; b) *ibid.* Appl. Phys. Lett. 88 (2006) 092110.
[4] P. Wahnón *et al.* J. Mater. Sci., 40 (2005) 1383.
[5] P. Palacios *et al.* Phys. Rev. B 73 (2006) 085206.
[6] P. Palacios *et al.* Thin Solid Films 515 (2007) 6280.
[7] J. Kambas *et al.* J. Phys. Stat. Sol. (b) 127 (1985) 201.
[8] P. Palacios *et al.*, Phys. Rev. Lett. 101 (2008) 046403. See also contribution 1CV.1.17 in this conference.
[9] (a) R. Lucena *et al.* Chem. Maters. 20 (2008) 5125. (b) Spanish Patent Application ES 200702008. Priority date: July 19th 2007
[10] G.A. Steigmann *et al.* Acta Cryst. 19 (1965) 967.
[11] (a) R. Diehl *et al.* J. Cryst. Growth 20 (1973) 38. (b) *ibid.* Acta Cryst. B 32 (1976) 1257. (c) K.J. Range *et al.* Z. Naturf. B 33 (1978) 463.
[12] G. Kresse *et al.* Phys. Rev. B 47 (1993) 558.
[13] P.E. Blöchl Phys. Rev. B 50 (1994) 17953.
[14] G. Kresse *et al.* Phys. Rev. B 59 (1999) 1758.
[15] B. Adolph *et al.* Phys. Rev. B 63 (2001) 125108; M. Gajdoš *et al.* Phys. Rev. B 73 (2006) 045112.
[16] P. Wahnón *et al.* Proc. 22nd Eur. Photovolt. Solar Eng. Conf., 56-59, 2007.
[17] C. Guillén *et al.* Thin Solid Films 451–452 (2004) 112.
[18] (a) C. Adenis *et al.* Rev. Chim. Minérale 24 (1987) 10. (b) JCPDS file 32-0456.
[19] M. Wakaki *et al.* Jap. J. Appl. Phys. 19 (1980, Sup. 19-3) 255
[20] E. Fortin *et al.* Solid St. Commun. 77 (1991) 165.
[21] a) F.G. Donika *et al.* Kristallografiya 15 (1971) 235; b) *ibid.* p. 813.
[22] T. Toyoda *et al.* Jpn. J. Appl. Phys. 32 (1993) 291
[23] K.J. Range *et al.* Z. Naturf. 24b (1969) 811.